THE JOURNAL OF BIOLOGICAL CHEMISTRY
Vol. 271, No. 36, Issue of September 6, pp. 21853–21858, 1996
Printed in U.S.A.

Stability and Oligomeric Equilibria of Refolded Interleukin-1β Converting Enzyme*

(Received for publication, April 3, 1996, and in revised form, June 6, 1996)

Robert V. Talanian‡, Luan C. Dang, Catherine R. Ferenz, Maria C. Hackett, John A. Mankovich, Jeffrey P. Welch, Winnie W. Wong, and Kenneth D. Brady

From BASF Bioresearch Corporation, Worcester, Massachusetts 01605

We report the preparation and characterization of interleukin-1β converting enzyme (ICE) refolded from its p20 and p10 protein fragments. Refolded ICE heterodimer (p20p10) was catalytically active but unstable, and in size exclusion chromatography eluted at an apparent molecular mass of 30 kDa. The mechanisms of the observed instability were pH-dependent dissociation at low enzyme concentrations, and autolytic degradation of the p10 subunit at high concentrations. Binding and subsequent removal of a high affinity peptidic inhibitor increased the apparent molecular mass to 43 kDa (by size exclusion chromatography), and significantly increased its stability and specific activity. Chemical cross-linking and SDS-polyacrylamide gel electrophoresis analysis of the 43-kDa size exclusion chromatography conformer revealed a 60-kDa species, which was absent in the 30-kDa conformer, suggesting that inhibitor binding caused formation of a $(p20p10)_2$ homodimer. The observation of a reversible equilibrium between ICE (p20p10) and $(p20p10)_2$ suggests that analogous associations, possibly between ICE and ICE homologs, can occur *in vivo*, resulting in novel oligomeric protease species.

Interleukin-1β converting enzyme (ICE)[1] (1, 2) is an intracellular cysteine protease that activates the proinflammatory cytokine interleukin-1β (IL-1β) by cleavage at Asp^{116}-Ala^{117} (3–5). Several lines of evidence suggest that ICE activity is required for IL-1β activation and that this is a crucial step in inflammation. IL-1β activation is effectively blocked by CrmA, a cowpox virus serpin that binds and inhibits ICE (6). The tetrapeptide ICE inhibitor acetyl-Tyr-Val-Ala-Asp-CHO (Ac-YVAD-CHO) (2) is also effective in blocking IL-1β activation (2, 7–9). Mice lacking functional copies of the murine ICE gene (10, 11), and cells derived from those animals, are deficient in IL-1β maturation. ICE-deficient mice are also resistant to endotoxic shock (10). These results suggest that inhibition of IL-1β activation by ICE is sufficient to block inflamation, and encourage efforts to develop ICE inhibitors as antiinflammatory drugs (12, 13).

Several human genes encoding proteins homologous to ICE have been discovered, and elucidation of the biological functions of these proteins is currently an active area of research. These include Ich-1 (14), TX/Ich-2/ICE_{rel}II (15–17), CPP32 (18), ICE_{rel}III (17), Mch2 (19), and Mch3/ICE-LAP3/CMH-1 (20–22). A clue to the function of ICE homologs, and possibly a second function of ICE itself, is provided by ced-3, a *Caenorhabditis elegans* protease that is highly homologous to ICE and is required for apoptosis (23, 24). The hypothesis that ICE or ICE homologs participate in apoptosis is supported by the antiapoptotic effects of CrmA and the baculovirus protein p35 (25, 26), which is also an inhibitor of ICE and ICE homologs, and by the observation that transient expression of antisense-ICE cDNA blocks Fas-induced apoptosis (27). Overexpression of ICE or many of its homologs in cultured cells causes apoptosis. Biochemical evidence suggests that in at least one model system CPP32 is required for apoptosis (28).

ICE is synthesized *in vivo* as an inactive 45-kDa proenzyme which is cleaved at three sites to generate p20 and p10 fragments, that together constitute the active form of the enzyme (2). The sequences at the cleavage sites correspond to the substrate specificity of ICE itself (Asp in P1) (13). This unusual specificity is shared only with ICE homologs and the serine protease granzyme B (29, 30), suggesting that ICE maturation is catalyzed by ICE itself or by related enzymes. Purified ICE p45 precursor protein can autoprocess *in vitro* to the active form of ICE (31), demonstrating that ICE processing can be autocatalytic and does not necessarily require a second protease.

Natural sources of active ICE provide insufficient material for crystallization and x-ray structure determination (2). To prepare material suitable for ICE crystallization we developed a protocol for refolding ICE p20 and p10 fragments that were separately expressed and purified from *Escherichia coli*. We favored this approach because we found that proteolytic processing of an ICE precursor led to proteolytic heterogeneity. Here we describe a method for refolding ICE, and the stability and mechanisms of degradation of the resulting material. The crystal structure of refolded ICE shows that it is a homodimer of (p20/p10) heterodimers (32). We observe that both (p20/p10) and homodimeric $(p20/p10)_2$ ICE are catalytically active, and that a simple equilibrium exists between these species, which is influenced by pH and the presence of peptidic ligands.

EXPERIMENTAL PROCEDURES

Materials—α-Pyridoin was obtained from Aldrich. Bovine serum albumin and bis-maleimidohexane were purchased from Sigma. Ac-Tyr-Val-Ala-Asp-Amc and Ac-Tyr-Val-Ala-Asp-CHO were obtained from Bachem Bioscience (Philadelphia, PA). Cell culture media were purchased from Difco (Detroit, MI).

Expression of ICE Fragments—Recombinant DNA sequences encoding ICE p20 and p10 were polymerase chain reaction subcloned into the *Eco*RI-*Spe*I site of a pBluescript II KS(+) (Strategene, La Jolla, CA) derivative (pJAM4) containing the bacteriophage l promoter (33) cloned

* The costs of publication of this article were defrayed in part by the payment of page charges. This article must therefore be hereby marked "*advertisement*" in accordance with 18 U.S.C. Section 1734 solely to indicate this fact.

‡ To whom correspondence and reprint requests should be addressed. Tel.: 508-849-2581; Fax: 508-754-7784; E-mail: talanian@biovax.dnet.basf-ag.de.

[1] The abbreviations used are: ICE, interleukin-1β converting enzyme; IL-1β, interleukin-1β; DTT, dithiothreitol; PAGE, polyacrylamide gel electrophoresis; SEC, size exclusion chromatography; Amc, aminomethylcoumarin; CHO, Chinese hamster ovary; Ac-YVAD-CHO, acetyl-Tyr-Val-Ala-Asp-CHO; Ac-YVAD-Amc, acetyl-Tyr-Val-Ala-Asp-Amc; rfICE, refolded ICE; Tricine, *B*-[2-hydroxy-1,1-bis(hydroxymethyl)ethyl] glycine.

into its unique *Xba*I site. The following polymerase chain reaction primers were used: P1 (p20 NH_2 terminus): 5′-GGG GAA TTC ATG AAC CCG GCT ATG CCG ACC TCT TCT GGT TCT GAA GGT AAC GTT AAA CTG TGC TCT CTG GAA GAA GC-3′; P2 (p20 COOH-terminus): 5′-CCC CAC TAG TCC TCT ATT AAT CTT TAA ACC ACA CCA CAC CAG GGC-3′; P3 (p10 NH_2 terminus): 5′-GGG GAA TTC ATG GCT ATC AAA AAA GCT CAC ATC GAA AAA GAC TTC ATC GCT TTC TGC-3′; P4 (p10 COOH terminus): 5′-CCC CAC TAG TCC TCT ATT AAT GTC CTG GGA AGA GG-3′. The resulting plasmids, pJAM4 ICE(120–297) and pJAM4 ICE(317–404) for p20 and p10, respectively, contain the genes under the control of the inducible pL promoter, with several altered amino-terminal codons that reflect *E. coli* codon preferences.

Expression vectors for ICE p10 or p20 were transfected into *E. coli* CAG597 cells (New England Biolabs, Beverly, MA) containing the temperature-sensitive repressor cI^{857} constitutively expressed from a gene inserted into the *Bgl*II-*Pst*I site of the vector pACYC177 (34). Cells were used to inoculate a 12.5-liter culture of EC3 medium at 29 °C in a 21-liter fermentor. EC3 medium contained the following in 12.5 liters: 225 g of tryptone, 75 g of yeast extract, 22 mM K_2HPO_4, 14 mM $(NH_4)_2SO_4$, 8 mM NaH_2PO_4, 1.5 g of ampicillin, and 0.75 g of kanamycin. The pH of the solution was maintained at 6.8 during the fermentation by addition of 15% NH_4OH as needed. 1.2 liters of EC3A medium was added gradually throughout the fermentation and induction periods. EC3A medium contained the following in 1.2 liters: 127 mM $MgSO_4$, 20 mM citric acid, 4 mM $Fe_2(SO_4)_3$, 4.7 mM $CaCl_2$, 2.6 mM $Zn(NO_3)_2$, 1.1 mM $MnCl_2$, 0.9 mM H_3BO_3, 0.57 mM $CuCl_2$, 0.23 mM $CoCl_2$, 0.23 mM Na_2MoO_4, and 50% (v/v) glycerine USP. One hour prior to induction and throughout the induction period, a solution of 1 liter of EC3B medium was added gradually. EC3B medium contained the following in 1 liter: 100 g of tryptone, 50 g of yeast extract, and 85 mM NaCl. Cells were grown at 29 °C to an OD_{600} value of 30, when the temperature was raised to 42 °C to induce protein synthesis. The cells were harvested 4 h after induction, and concentrated using a Pellicon filter unit (Millipore, Bedford, MA) with a 0.2-μm tangential filter, followed by centrifugation at 12,000 × *g* for 30 min. The supernatant was removed, and the cell pellets were stored at −80 °C.

Cells were lysed and homogenized by suspending in 4 liters of lysis buffer (50 mM Tris and 2% (v/v) Triton X-100, at pH 8.0) at 4 °C, and passing twice through a microfluidizer. The sample was diluted to 5.5 liters with lysis buffer, incubated at room temperature with stirring for 60 min, and centrifuged at 12,000 × *g* for 20 min at room temperature. The pellet was then twice resuspended in 5.5 liters of fresh lysis buffer, incubated, and centrifuged. This was repeated twice using a buffer that contained 500 mM NaCl and 50 mM Tris at pH 8.0, and then once with 50 mM Tris at pH 8.0. Approximately 800 g (wet weight) each of inclusion bodies were obtained for p10 and p20.

Purification and Refolding of ICE Fragments—Inclusion bodies were dissolved in a solution of 6 M guanidine hydrochloride, 200 mM DTT, and 50 mM Tris, at pH 8.5, at approximately 1 mg ml^{-1} (p10) or 2 mg ml^{-1} (p10). Samples were dialyzed *versus* 5% HOAc at room temperature, centrifuged at 27,000 × *g* for 40 min, then filtered at 0.22 μM. Samples were purified by high performance liquid chromatography using a reverse phase C_8 (p10) or C_4 (p20) column (Vydac) and a linear gradient of CH_3CN-H_2O with 0.1% (v/v) trifluoroacetic acid. Final yield was approximately 1.5 g of lyophilized protein. Electrospray ionization mass spectrometry (M-Scan, West Chester, PA): p20, calculated (with initiator methionine present), 19,974; found, 19,987; p10, calculated (with initiator methionine absent), 10,243; found, 10,243.

ICE p20 and p10 fragment proteins were dissolved at approximately 2 mg ml^{-1} in solutions containing 6 M guanidine hydrochloride and 200 mM DTT at pH 8.5, by overnight incubation at room temperature, and the protein concentrations were measured by amino acid analysis. Protein solutions were mixed at a 1:1 molar ratio and a final protein concentration of 50–250 μg ml^{-1} as indicated in a solution containing 6 M guanidine hydrochloride, 25 mM Tris, 5 mM DTT, 0.5 mM EDTA, at pH 9.0. The mixture was dialyzed (Spectra-Por 1, 6–8000 MWCO, 1 ml cm^{-1}) *versus* 2 changes of 100 volumes of a solution containing 25 mM Tris, 5 mM DTT, 0.5 mM EDTA, at pH 9.0, and 4 °C for a minimum of 3 h each. The protein solution was then dialyzed *versus* 1 change of 100 volumes of a solution containing 100 mM HEPES, 20% (v/v) glycerol, 5 mM DTT, 0.5 mM EDTA, at pH 6.7, for a total of 3 h. The pH of the resulting solution was adjusted to 7.0 by dropwise addition of 2 M HEPES at pH 5.5, and the sample was centrifuged at 2,200 × *g* and filtered at 0.22 μm.

The resulting catalytically active enzyme mixture was further purified by fast protein liquid chromatography using a MonoS HR16/10 cation exchange column (Pharmacia, Uppsala, Sweden) equilibrated in Buffer A (50 mM HEPES, 20% glycerol, and 0.5 mM EDTA, pH 6.7) at 4 °C, and eluted with a linear gradient of Buffer A/Buffer A plus 0.5 M NaCl.

Determination of Protein Concentration—Protein concentrations were determined by Coomassie Plus staining (Pierce) using bovine serum albumin as a standard.

ICE Activity Assays—Refolded ICE was diluted to the indicated concentrations into 400 μl of HGDE buffer (100 mM HEPES, pH 6.7, 5 mM DTT, 0.5 mM EDTA, 20% glycerol), plus 15 μM acetyl-Tyr-Val-Ala-Asp-Amc (Ac-YVAD-Amc) (35) in a 2 × 10-mm fluorescence cuvette at 37 °C. The change in fluorescence due to liberated Amc was monitored at 460 nm using 380 nm excitation in a LS-50B Luminescence Spectrometer (Perkin-Elmer, Norwalk, CT). Standard curves were prepared using solutions of Amc in assay buffer.

Assays at low enzyme concentrations demonstrated distinct biphasic behavior, with a period of downward curvature followed by a linear steady-state. Therefore, results were modeled by non-linear regression an equation describing the transition to equilibrium:

$$F(t) = F_0 + V_f t + (V_i - V_f)(1 - e^{-kt})/k \qquad \text{(Eq. 1)}$$

where F_0 is the fluorescence at $t = 0$, V_i and V_f are initial and final velocities, and k is the first-order rate constant describing decay of ICE activity.

Size Exclusion Chromatography—Analytical size exclusion chromatography (SEC) of ICE was performed using a SMART System (Pharmacia, Uppsala, Sweden) with a Superdex-75 column (3.2 × 300 mm, 2.0-ml bed volume) at 6 °C with PBS buffer at 45 μl min^{-1}. Injection volumes were ≤50 μl. Absorbance of the column eluate was monitored at 280 and 230 nm, and signals at these wavelengths were proportional. Molecular weights of experimental peaks were evaluated from plots of $\log(M_r)$ *versus* elution time for comparable standard proteins (Pharmacia LKB Biotech). Peak areas were evaluated using non-linear regression analysis to fit chromatograms to an expression for two independent Gaussian curves:

$$\frac{A_1}{\sigma_1\sqrt{2\pi}}\exp\left[\left(\frac{t-m_1}{4\sigma_1}\right)^2\right] + \frac{A_2}{\sigma_2\sqrt{2\pi}}\exp\left[\left(\frac{t-m_2}{4\sigma_2}\right)^2\right] \qquad \text{(Eq. 2)}$$

pH-dependence of rfICE Stability—Buffers in the pH range 6.0–8.0 were prepared by adjusting a stock HGDE buffer to the given pH by addition of 1 N HCl or NaOH. Aliquots of refolded ICE were thawed, and enzyme was diluted to a final concentration of 1 nM into the buffers containing 15 μM Ac-YVAD-Amc. Fluorescence was monitored for 1000 s, or until steady-state was achieved. Data were fitted to Equation 1 by non-linear regression analysis.

Cross-linking of Refolded ICE—Refolded ICE (0.8 μM) was thawed and a 1-ml aliquot was treated either with 100 μM Ac-YVAD-CHO (Bachem Bioscience, Philadelphia, PA) for 30 min at 25 °C or with 200 μM α-pyridoin for 1 h at 25 °C. Reactions were cooled to 4 °C, and solid ammonium sulfate (J. T. Baker, Phillipsburg, NJ) was added to the reactions to achieve 80% saturation. The samples were incubated on ice for 2 h, then centrifuged at 13,000 × *g* for 20 min. Pellets were resuspended gently with 25 μl of HGE buffer (HGDE without DTT), then centrifuged to remove aggregated protein. Concentrated inhibited enzyme samples were analyzed by size exclusion chromatography as described above. The major fraction (22.5 μl) at 43 kDa (Ac-YVAD-CHO-inhibited enzyme) or at 29 kDa (α-pyridoin-inhibited enzyme) was collected and treated with 250 μM bis-maleimidohexane (Pierce) at 25 °C for 45 min. The reactions were then rechromatographed on Superdex-75. Small fractions were collected, chromatographed on 10–20% Tris-Tricine mini gel (Integrated Separation Systems, Natick MA), and detected by silver staining.

Reactivation of Ac-YVAD-CHO-inhibited Refolded ICE—An aliquot of frozen refolded ICE (25 mg ml^{-1}) was thawed to 4 °C, and Ac-YVAD-CHO was added to a final concentration of 200 μM. The sample was warmed to room temperature and incubated for 30 min. The mixture was then dialyzed exhaustively at room temperature against 100 mM HEPES, pH 6.7, 20% glycerol, 0.5 mM EDTA, 25 mM semicarbazide, 5 mM glutathione disulfide, with three buffer changes over 12 h, and a final 1 h dialysis at 4 °C into HGE. The enzyme was stored at −80 °C until ready for use.

RESULTS

Preparation of Refolded ICE—The p20 and p10 subunits corresponding to the active form of ICE (2) were expressed separately in *E. coli* from pL-based vectors as insoluble inclusion bodies. After inclusion body purification and reverse phase

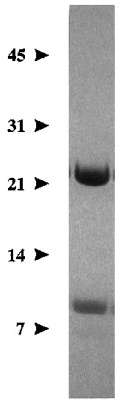

FIG. 1. **SDS-PAGE analysis of purified ICE refolded from the p20 and p10 subunits.** A sample containing approximately 5 μg of rfICE was electrophoresed on a 10–20% Tris-Tricine gradient gel, and protein was detected using Coomassie Blue staining. Molecular weight standards are as indicated.

high performance liquid chromatography, approximately 1.5 g of lyophilized proteins at 80–90% purity were obtained from 14-liter fermentations. The purified proteins were dissolved in a reducing and denaturing Tris buffer at pH 9.0, and mixed at a 1:1 molar ratio at 250 μg ml^{-1}. Catalytically active ICE enzyme was prepared by refolding the p20 and p10 fragments as described under "Experimental Procedures." Refolding was effected by exhaustive dialysis first against a similar buffer lacking denaturant. To generate active enzyme, the material was then dialyzed against a buffer containing HEPES at pH 6.7. Dialysis of denatured p20 and p10 directly into the HEPES buffer resulted in catalytically inactive material.

Refolded ICE (rfICE) was purified by ion exchange chromatography to >95% as judged by SDS-PAGE (Fig. 1), with a single significant contaminant at about 7 kDa (p7). NH_2-terminal sequencing identified p7 as a degradation product of ICE p10 arising from cleavage at Asp^{381}-Gly^{382}. Complex formation with the irreversible peptidic ligand acetyl-Tyr-Val-Ala-Asp-CMK (32) altered the ion exchange mobility of rfICE, but the observation that only half of the material displayed altered mobility after incubation with saturating amounts of peptidic ligand suggested that rfICE contained approximately 50% catalytically inactive protein.

Stabilization of rfICE by Substrate—When rfICE catalytic activity was assayed at a protein concentration of 3 nM, the rate of catalysis decreased for approximately 100 s to a constant non-zero velocity (Fig. 2*A*). Equation 1 was used to derive initial and final velocities and rate constants for this process as a function of substrate concentration. Michaelis-Menton analysis of the initial velocities (Fig. 2*B*) gave K_m and k_{cat} values of 8 μM and 0.05 s^{-1}, respectively. The observed k_{cat} for rfICE is about 10-fold less than that reported for ICE purified from human THP.1 monocytes (2). The plot of final velocities (Fig. 2*B*) is sigmoidal, reflecting a substrate-induced decrease in the rate of the rapid decay phase. This is further illustrated by the effect of substrate concentration on the decay rate constant (Fig. 2*C*). Since the ratio $K_m/(S+K_m)$ provides a measure of the total enzyme in the unbound state, the decay rate as a function of substrate concentration can be modeled by:

$$k \approx k_{inact} + k_{unbound}K_m(S + K_m)(\text{for } k_{inact} \ll k_{unbound}) \quad \text{(Eq. 3)}$$

where k_{inact} is the rate of decay by some process that affects all enzyme and $k_{unbound}$ is the rate of decay of enzyme with no bound ligand. Fitting the data of Fig. 2*C* to Equation 3 yielded $k_{unbound}$ = 0.040 s^{-1}, k_{inact} = 0.0021 s^{-1}, and K_m = 5.5 μM. By this model, substrate binding decreases the decay rate of rfICE 20-fold. The initial slope (*i.e.* for [S] < 10 μM) of the plot of final

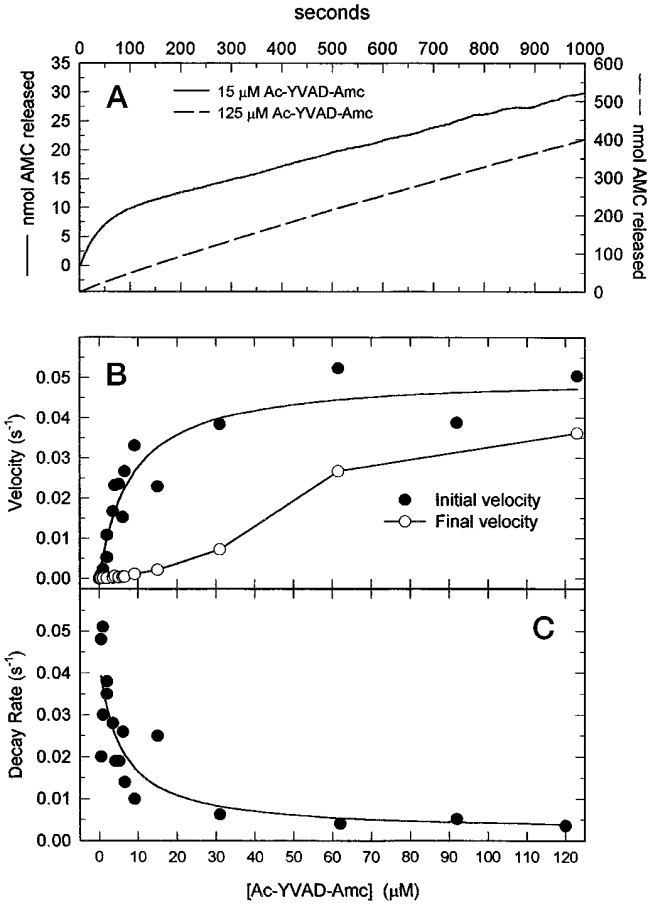

FIG. 2. **Stabilization of rfICE by substrate.** *A*, rfICE was assayed at 15 or 125 μM Ac-YVAD-Amc as described under "Experimental Procedures." *B*, substrate concentration was varied up to 125 μM, and initial and final velocities were obtained by fitting the assay curves to Equation 1. The *solid curve* describing initial velocities represents a fit to the Michaelis-Menton equation with K_m = 8 μM and k_{cat} = 0.05 s^{-1}. *C*, rate constants from *B* are plotted as a function of substrate concentration. The *solid line* represents a fit to Equation 3 with k_{free} = 0.040 s^{-1}, k_{bound} = 0.0021 s^{-1}, and K_m = 5.5 μM.

velocities is 65 M^{-1} s^{-1}, while that of the final velocities is 6250 M^{-1} s^{-1}. Thus, at low substrate concentrations, the specific activity of rfICE falls to approximately 1% of its initial value.

Enzyme Concentration Dependence of rfICE Decay—At low enzyme concentrations, decay of rfICE activity was monitored by reaction progress curves (Fig. 3*A*). Below 10 nM, activity fell quickly (k = 0.02–0.04 s^{-1}; $t_{½}$ < 40 s) to a low steady-state value (Fig. 3*A*, *inset*). As enzyme concentration was increased toward 24 nM, activity loss became slower, with time constants approaching 0.0035 s^{-1}. When refolded enzyme was preincubated at 37 °C at four different concentrations in the range 50–2000 nM, velocities fell to a final non-zero value with a time constant of 0.0023 ± 0.0008 s^{-1} ($t_{½}$ = 5 min; Fig. 3*B*). There was no observable dependence of decay rate on enzyme concentration in this range. The combined plot of decay rates *versus* enzyme concentration for both types of experiments (Fig. 3*B*, *inset*) shows that the decay rate is concentration-dependent for [E] < 30 nM, and concentration-independent up to 2 μM.

The contribution of proteolysis to enzyme decay was tested by incubating 2 μM rfICE for various times followed by SDS-PAGE analysis. Over 1 h, the intensity of the 10-kDa band decreased, accompanied by the appearance of lower molecular weight fragments (Fig. 3*C*). The disappearance of ICE p10 correlated with activity loss (Fig. 3*D*). We conclude that autolytic cleavage of the 10-kDa subunit is the primary process of rfICE inactivation at high (≥2 μM) enzyme concentrations,

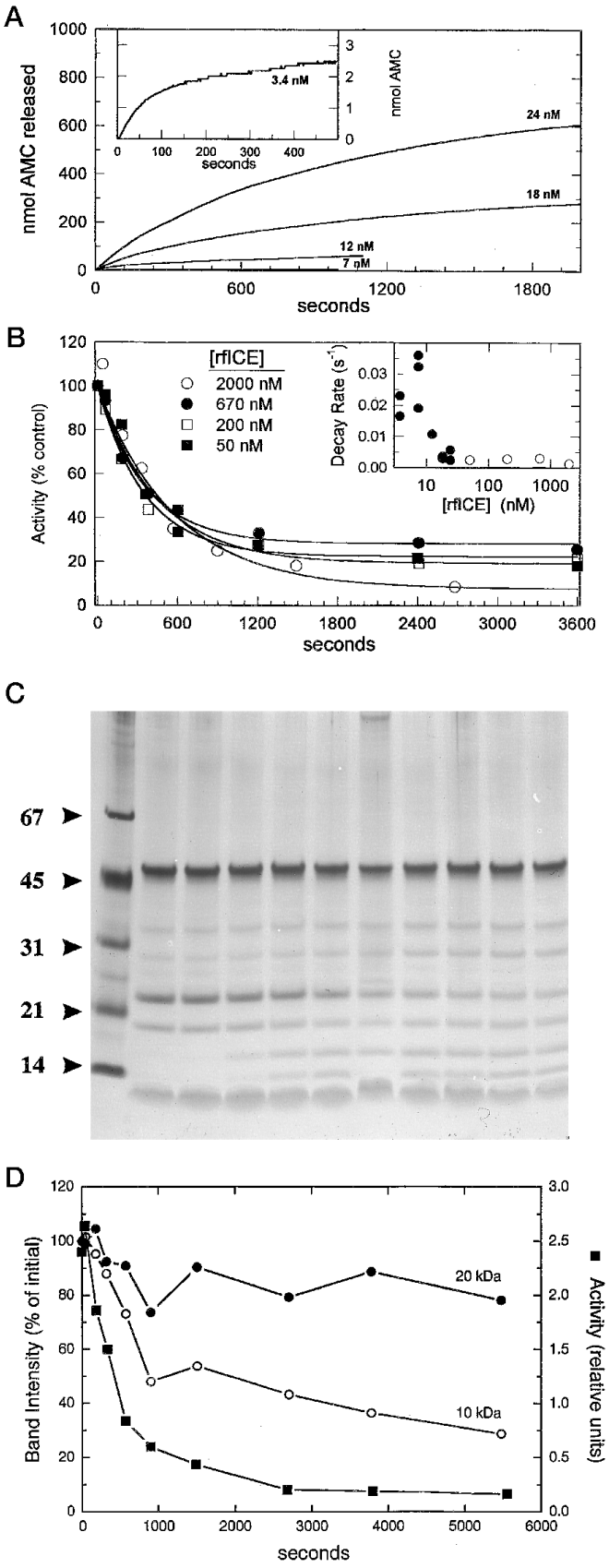

FIG. 3. **Enzyme concentration dependence of rfICE decay.** *A*, rfICE was diluted to nominal concentrations of 3.4 (*inset*), 7, 12, 18, or 24 nM as indicated, into HGDE buffer containing 15 μM Ac-YVAD-Amc. Substrate hydrolysis was followed for 2000 s (18 and 24 nM concentrations), or until steady-state was achieved (3, 7, and 12 nM; see *inset*). Curves were fit to Equation 1 to estimate the decay rates (see inset to *B*). *B*, rfICE was diluted into HGDE buffer (pH 7.5, 30 °C) to the indicated nominal concentrations. Aliquots were withdrawn at the indicated times and diluted into HGDE (pH 7.5) buffer containing 15 μM Ac-YVAD-Amc. Substrate hydrolysis was linear at pH 7.5, and reactions were followed for 30 (control assay) or 60 s. Velocities were obtained by linear regression analysis. All rates are reported as a percentage of the control rate obtained 5 s after dilution. Activity decayed to a final non-zero rate, so that rate constants were estimated by fitting to the model $A(t) = A_{final} + (100 - A_{final})e^{-kt}$, where A_{final} is the velocity at large times, and k is the rate of decay. *Inset B*, decay rate constants observed from reaction progress curves (*solid circles*) or preincubation assays (*open circles*) are plotted as a function of enzyme concentration. *C*, SDS-PAGE analysis of room temperature-incubated rfICE. Lanes represent samples drawn at various times as indicated in *panel D*. Molecular weight standards are as shown. *D*, band intensities of rfICE p20 (*closed circles*) and p10 (*open circles*) from the gel of *panel C* were quantitated by scanning, and are plotted against the catalytic activity (*closed squares*) of the same samples in standard assays.

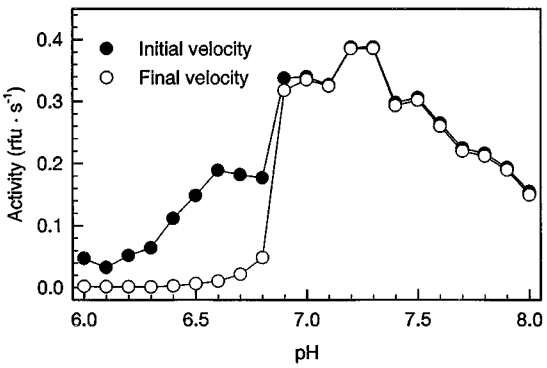

FIG. 4. **pH dependence of rfICE stability.** HGDE buffers were prepared over the pH range 6.0–8.0 as described under "Experimental Procedures." Substrate Ac-YVAD-Amc was added to 15 μM, and refolded ICE was added to 1 nM. Activity was monitored for 1000 s or until a steady-state velocity was achieved. Progress curves were modeled to Equation 1 using non-linear regression, and the initial (*closed circles*) and final (*open circles*) velocities are plotted as a function of pH.

while dissociation is the primary process at low (<30 nM) concentrations.

pH Dependence of rfICE Inactivation—The pH dependence of the rapid phase of rfICE decay at low rfICE concentration (1 nM) was examined using a series of HEPES buffers from pH 6.0 to 8.0. The enzyme was assayed using 15 μM Ac-YVAD-Amc, and the resulting curves were analyzed using Equation 1. At the lower pH values, activity decayed rapidly to final, very low values (Fig. 4). Between pH 6.8 and 6.9, a dramatic increase in the stability of the enzyme was observed, and at pH values >6.9, little or no rapid decay occurred. We conclude that ionizations with pK_a values <6.9 greatly affect the physical stability of rfICE. The steepness of the transition suggests that several ionizations are involved.

Analytical Size Exclusion Chromatography of Refolded ICE—Two distinct species within rfICE were resolved by analytical SEC, at apparent molecular masses of 43 and 29 kDa (Fig. 5*A*). The areas under each peak were estimated to be 6 and 94%, respectively, using Equation 2. A disproportionately high fraction of total catalytic activity coincided with the higher molecular weight peak. Exposure of rfICE to 200 μM of the reversible peptidic inhibitor Ac-YVAD-CHO (2) for 150 s at 4 °C changed the distribution of protein such that 43% of the protein eluted at 43 kDa (Fig. 5*A*). A similar shift was also induced by the irreversible inhibitor Ac-YVAD-CMK (32) (data not shown). The mobility shift persisted when rfICE was treated with 200 μM Ac-YVAD-CHO for 30 min, then dialyzed exhaustively against HGE buffer containing 5 mM oxidized glutathione and 25 mM semicarbazide to remove the inhibitor. The resulting material (Fig. 5*B*) migrated predominantly as the 43-kDa species containing almost all of the enzyme activity. We conclude

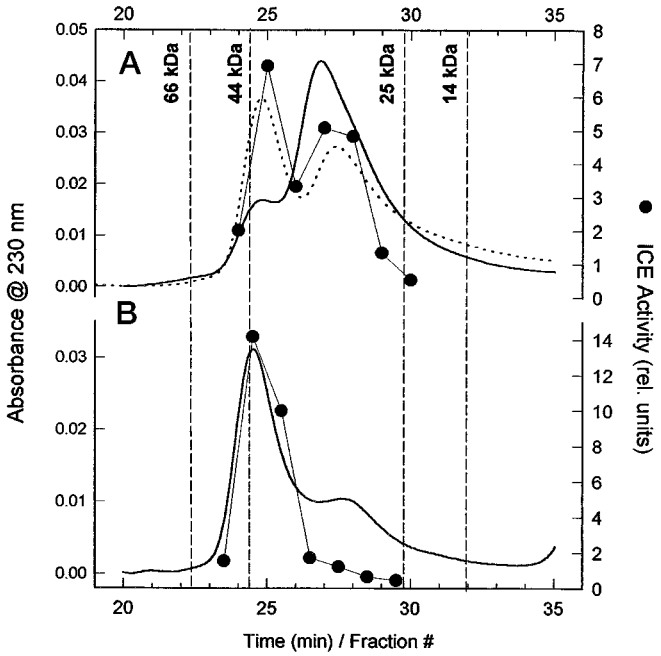

FIG. 5. **Size exclusion chromatography analysis of rfICE.** rfICE was analyzed by SEC as described under "Experimental Procedures." *A*, elution of uninhibited (*solid line*) or Ac-YVAD-CHO inhibited (*dashed line*) rfICE. Fractions of untreated rfICE were collected and assayed in HGDE as described under "Experimental Procedures" using 15 μM Ac-YVAD-Amc (*solid circles*). Elution of molecular weight standards (Pharmacia LKB Biotechnology) bovine serum albumin (67 kDa), ovalbumin (43 kDa), chymotrypsinogen A, (25 kDa), and ribonuclease A (13 kDa) were as indicated. *B*, elution and activity assay of rfICE inhibited with Ac-YVAD-CHO followed by inhibitor removal.

that binding of a peptidic inhibitor favors the formation of a higher order oligomer of rfICE, which displays significantly increased stability and specific activity.

Cross-linking and SDS-PAGE Reveal a 60-kDa ICE Species—Refolded ICE in complex with Ac-YVAD-CMK (32) or Ac-YVAD-CHO[2] crystallized as a 60-kDa tetramer, but migrated at about 43 kDa in analytical SEC. Although anomalous protein SEC mobility is common, cross-linking studies were performed to resolve this discrepancy. rfICE was treated with Ac-YVAD-CHO or α-pyridoin, a light-dependent ICE inhibitor that fails to induce an SEC mobility shift. The samples were concentrated by $AmSO_4$ precipitation, purified by SEC, and cross-linked with bis-maleimidohexane. The material was then repurified by SEC. SDS-PAGE analysis with silver staining revealed a 60-kDa species in the 43-kDa SEC fractions resulting from Ac-YVAD-CHO treatment (Fig. 6*A*). The strong band at about 43 kDa may represent a partially cross-linked species. The 29-kDa SEC fraction from Ac-YVAD-CHO treated rfICE contained among others a prominent 30-kDa species but no 60-kDa species. The 60-kDa band was similarly absent from all fractions of ICE that had been treated with α-pyridoin prior to cross-linking (Fig. 6*B*). We conclude that rfICE migrating by SEC at an apparent molecular mass of 43 kDa is at least partially composed of the expected $(p20p10)_2$ 60-kDa tetramer, which migrates on SEC at an anomalously low apparent molecular mass. Catalytically active material that migrates at about 29 kDa contains the expected (p20p10) heterodimer.

DISCUSSION

Our data suggests that active rfICE exists in an equilibrium between (p20p10) heterodimer and a $(p20p10)_2$ homodimer of

[2] N. P. C. Walker, R. V. Talanian, L. C. Dang, C. R. Ferenz, M. C. Hackett, J. A. Mankovich, J. P. Welch, W. W. Wong, and K. D. Brady, unpublished results.

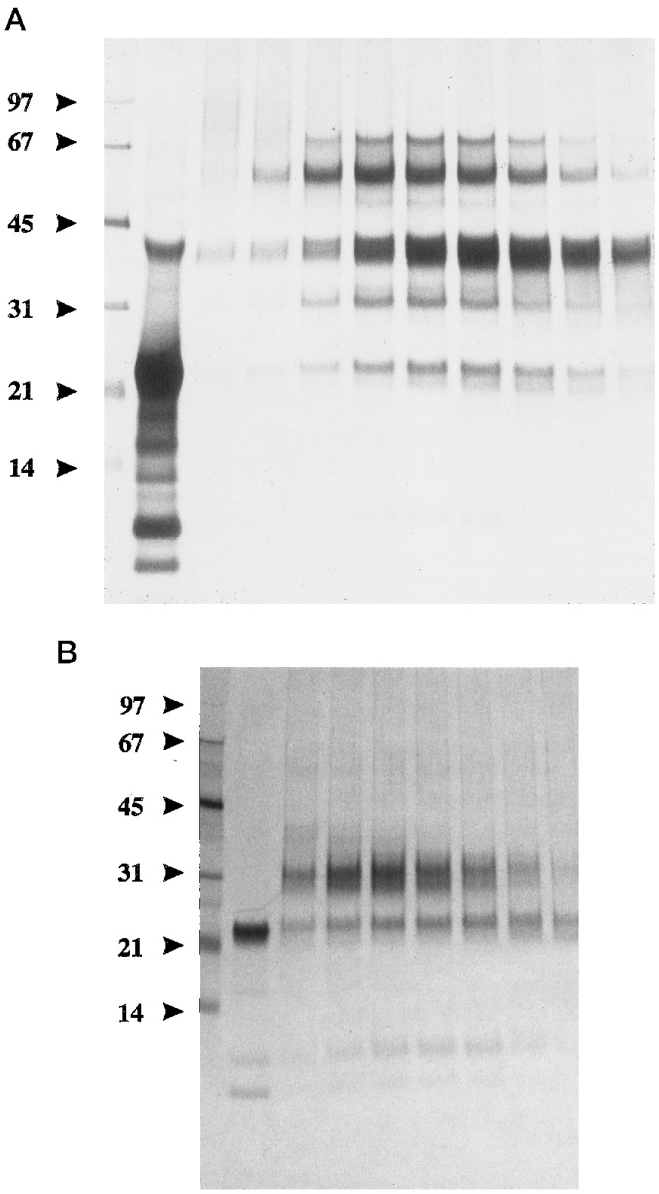

FIG. 6. **Identification of a 60-kDa ICE species in the 43-kDa SEC peak.** *A*, refolded ICE was treated with Ac-YVAD-CHO (100 μM) for 30 min at 25 °C, precipitated by addition of solid ammonium sulfate, centrifuged, and redissolved in 25 μl of HGE, and separated by SEC as described under "Experimental Procedures." The major peak at 43 kDa was treated with bis-maleimidohexane (250 μM) for 45 min at room temperature. The mixture was rechromatographed by SEC, and fractions were collected and analyzed by SDS-PAGE. *Lane 1*, molecular weight standards. *Lane 2*, ammonium sulfate-concentrated rfICE prior to separation by SEC. *Lanes 3–11*, fractions of the 43-kDa SEC peak. *B*, the same procedure was followed, except enzyme was inhibited using α-pyridoin, and the dominant SEC peak at 29 kDa was collected for cross-linking. *Lane 1*, molecular weight standards. *Lane 2*, rfICE control. *Lanes 3–9*, fractions of the 29-kDa SEC peak.

heterodimers. Enzyme decay occurs by at least two mechanisms: at high concentration, by autolytic cleavage, and at low concentration, by dissociation to heterodimers of low specific activity or to individual, catalytically inactive p20 and p10 subunits. The reversibility of the equilibrium between (p20p10) and $(p20p10)_2$ is supported by several lines of evidence: (i) the rapid decay of enzyme activity on dilution into assay mixtures is inversely proportional to final enzyme concentration, (ii) diluted enzyme activity reaches a stable non-zero level, and (iii) the decay fits well to a model for a reversible equilibrium (Equation 1). In addition, when rfICE binds a peptidic inhibitor

such as Ac-YVAD-CHO, the equilibrium between heterodimer and homodimer shifts toward homodimer (Fig. 5). The observation that high substrate concentrations stabilize and increase the specific activity of rfICE suggests that substrates also favor $(p20p10)_2$ formation, but we were unable to demonstrate formation of a 43-kDa species when rfICE was treated with high concentrations (≥1 mM) of peptide substrate followed by SEC analysis (not shown). We postulate that efficient formation of $(p20p10)_2$ occurs only when a long-lived enzyme-ligand complex is formed, as expected for slowly reversible (Ac-YVAD-CHO) or irreversible (Ac-YVAD-CMK) inhibitors.

In monocytes, ICE exists primarily as its p45 precursor form (36), suggesting that the mature, active form, when it is produced, decays rapidly. We observe that treatment of ICE with the peptide aldehyde inhibitor Ac-YVAD-CHO, followed by its removal, confers to the enzyme significantly enhanced stability. Purification of ICE from THP.1 cells using a peptide aldehyde affinity column (2) mimics our Ac-YVAD-CHO treatment. The stability of Ac-YVAD-CHO-treated rfICE is similar to that of THP.1 ICE (2). Thus the observed stability of isolated natural enzyme may be partly a result of the purification procedure.

The mechanism of ICE down-regulation *in vivo* is unknown. ICE contains numerous sites in its primary sequence that might be cleaved by ICE or ICE homologs. We find that Asp^{381}, within the p10 subunit, is the dominant site of autocleavage *in vitro*. Cleavage at this site is sufficient to inactivate ICE, as shown in Fig. 3*D*. We propose that D381 functions as a built in "off switch" for down-regulation of ICE *in vivo*. We also observe substantial substrate stabilization of ICE *in vitro*. It is tempting to speculate from this that ICE depends on IL-1β or other substrates for stability *in vivo* as well. If so, this may ensure that ICE remains active only when its substrate has been induced, and does not accumulate, leading inappropriately to apoptosis.

Our data shows that ICE (p20p10) heterodimer is in equilibrium with $(p20p10)_2$ homodimer. If this occurs *in vivo*, it would allow in principle the formation of pairs of (p20p10) heterodimers derived from two different gene products, most likely ICE homologs. Gu *et al.* (37) report evidence for domain swapping between ICE and the ICE homolog TX/Ich-2/ICE_{rel}II (15–17), which results in each (p20p10) heterodimer containing p20 from one gene product and p10 from another. Similarly, Fernandes-Alnemri *et al.* (20) present evidence for a complex of Mch3 and CPP32. Together with our data, these observations suggest that it is possible to form active ICE-like proteases derived from two to four separate gene products. The crystal structure of ICE shows that catalytic residues are part of p20, while the residues that form the P1-P4 pockets derive from both subunits. The many combinations of $(p20p10)_2$ that could be formed from ICE and its six known homologs may vary in their substrate specificities, catalytic properties, and control mechanisms. It is possible that different combinations of heterooligomeric species are stabilized by different natural substrates, offering further control of ICE-like enzyme formation and stability. Such fine control may be necessary for proper regulation of a family of enzymes responsible for both host defense and cellular suicide.

REFERENCES

1. Cerretti, D. P., Kozlosky, C. J., Mosley, B., Nelson, N., Van, N. K., Greenstreet, T. A., March, C. J., Kronheim, S. R., Druck, T., Cannizzaro, L. A., Huebner, K., and Black, R. A. (1992) *Science* **256,** 97–100
2. Thornberry, N. A., Bull, H. G., Calaycay, J. R., Chapman, K. T., Howard, A. D., Kostura, M. J., Miller, D. K., Molineaux, S. M., Weidner, J. R., Aunins, J., Elliston, K. O., Ayala, J. M., Casano, F. J., Chin, J., Ding, G. J.-F., Egger, L. A., Gaffney, E. P., Limjuco, G., Palyha, O. C., Raju, S. M., Rolando, A. M., Salley, J. P., Yamin, T.-T., Lee, T. D., Shively, J. E., MacCross, M., Mumford, R. A., Schmidt, J. A., and Tocci, M. J. (1992) *Nature* **356,** 768–774
3. March, C. J., Mosley, B., Larsen, A., Cerretti, D. P., Braedt, G., Price, V., Gillis, S., Henney, C. S., Kronheim, S. R., Grabstein, K., Conlon, P. J., Hopp, T. P., and Cosman, D. (1985) *Nature* **315,** 641–647
4. Cameron, P., Limjuco, G., Rodkey, J., Bennett, C., and Schmidt, J. A. (1985) *J. Exp. Med.* **162,** 790–801
5. Mosley, B., Urdal, D. L., Prickett, K. S., Larsen, A., Cosman, D., Conlon, P. J., Gillis, S., and Dower, S. K. (1987) *J. Biol. Chem.* **262,** 2941–2944
6. Ray, C. A., Black, R. A., Kronheim, S. R., Greenstreet, T. A., Sleath, P. R., Salvesen, G. S., and Pickup, D. J. (1992) *Cell* **69,** 597–604
7. Molineaux, S. M., Casano, F. J., Rolando, A. M., Peterson, E. P., Limjuco, G., Chin, J., Griffin, P. R., Calaycay, J. R., Ding, G. J., Yamin, T. T., Palyha, O. C., Luell, S., Fletcher, D., Miller, D. K., Howard, A. D., Thornberry, N. A., and Kostura, M. J. (1993) *Proc. Natl. Acad. Sci. U. S. A.* **90,** 1809–1813
8. Fletcher, D. S., Agarwal, L., Chapman, K. T., Chin, J., Egger, L. A., Limjuco, G., Luell, S., MacIntyre, D. E., Peterson, E. P., Thornberry, N. A., and Kostura, M. J. (1995) *J. Interferon Cytokine Res.* **15,** 243–248
9. Elford, P. R., Heng, R., L., R., and MacKenzie, A. R. (1995) *Br. J. Pharmacol.* **115,** 601–606
10. Li, P., Allen, H., Banerjee, S., Franklin, S., Herzog, L., Johnston, C., McDowell, J., Paskind, M., Rodman, L., Salfeld, J., Towne, E., Tracey, D., Wardwell, S., Wei, F.-Y., Wong, W., Kamen, R., and Seshadri, T. (1995) *Cell* **80,** 401–411
11. Kuida, K., Lippke, J. A., Ku, G., Harding, M. W., Livingston, D. J., Su, M. S., and Flavell, R. A. (1995) *Science* **267,** 2000–2003
12. Thornberry, N. A., Miller, D. K., and Nicholson, D. W. (1995) *Perspect. Drug Disc. Des.* **2,** 389–399
13. Miller, D. K., Calaycay, J. R., Chapman, K. T., Howard, A. D., Kostura, M. J., Molineaux, S. M., and Thornberry, N. A. (1993) *Ann. N. Y. Acad. Sci.* **696,** 133–148
14. Wang, L., Miura, M., Bergeron, L., Zhu, H., and Yuan, J. (1994) *Cell* **78,** 739–750
15. Faucheu, C., Diu, A., Chan, A. W. E., Blanchet, A., Miossec, C., Hervé, F., Collard-Dutilleul, V., Gu, Y., Aldape, R. A., Lippke, J. A., Rocher, C., Su, M. S., Livingston, D. J., Hercend, T., and Lalanne, J. (1995) *EMBO J.* **14,** 1914–1922
16. Kamens, J., Paskind, M., Hugunin, M., Talanian, R. V., Allen, H., Banach, D., Bump, N., Hackett, M., Johnston, C. G., Li, P., Mankovich, J. A., Terranova, M., and Ghayur, T. (1995) *J. Biol. Chem.* **270,** 15250–15256
17. Munday, N. A., Vaillancourt, J. P., Ali, A., Casano, F. J., Miller, D. K., Molineaux, S. M., Yamin, T.-T., Yu, V. L., and Nicholson, D. W. (1995) *J. Biol. Chem.* **270,** 15870–15876
18. Fernandes-Alnemri, T., Litwack, G., and Alnemri, E. S. (1994) *J. Biol. Chem.* **269,** 30761–30764
19. Fernandes-Alnemri, T., Litwack, G., and Alnemri, E. S. (1995) *Cancer Res.* **55,** 2737–2742
20. Fernandes-Alnemri, T., Takahashi, A., Armstrong, R., Krebs, J., Fritz, L., Tomaselli, K. J., Wang, L., Yu, Z., Croce, C. M., Salveson, G., Earnshaw, W. C., Litwack, G., and Alnemri, E. S. (1995) *Cancer Res.* **55,** 6045–6052
21. Duan, H., Chinnaiyan, A. M., Hudson, P. L., Wing, J. P., He, W.-W., and Dixit, V. M. (1996) *J. Biol. Chem.* **271,** 1621–1625
22. Lippke, J. A., Gu, Y., Sarnecki, C., Caron, P. R., and Su, M. S.-S. (1996) *J. Biol. Chem.* **271,** 1825–1828
23. Yuan, J., Shaham, S., Ledoux, S., Ellis, H. M., and Horvitz, H. R. (1993) *Cell* **75,** 641–652
24. Hugunin, M., Quintal, L. J., Mankovich, J. A., and Ghayur, T. (1996) *J. Biol. Chem.* **271,** 3517–3522
25. Bump, N. J., Hackett, M., Hugunin, M., Seshagiri, S., Brady, K., Chen, P., Ferenz, C., Franklin, S., Ghayur, T., Li, P., Licari, P., Mankovich, J., Shi, L., Greenberg, A. H., Miller, L. K., and Wong, W. W. (1995) *Science* **269,** 1885–1888
26. Miura, M., Zhu, H., Rotello, R., Hartweig, E. A., and Yuan, J. (1993) *Cell* **75,** 653–660
27. Los, M., Van de Craen, M., Penning, L. C., Schenk, H., Westendorp, M., Baeuerle, P. A., Dröge, W., Krammer, P. H., Fiers, W., and Schulze-Osthoff, K. (1995) *Nature* **375,** 81–83
28. Nicholson, D. W., Ali, A., Thornberry, N. A., Vaillancourt, J. P., Ding, C. K., Gallant, M., Gareau, Y., Griffin, P. R., Labelle, M., Lazebnik, Y. A., Munday, N. A., Raju, S. M., Smulson, M. E., Yamin, T.-T., Yu, V. L., and Miller, D. K. (1995) *Nature* **376,** 37–43
29. Odake, S., Kam, C. M., Narasimhan, L., Poe, M., Blake, J. T., Krahenbuhl, O., Tschopp, J., and Powers, J. C. (1991) *Biochemistry* **30,** 2217–2227
30. Poe, M., Blake, J. T., Boulton, D. A., Gammon, M., Sigal, N. H., Wu, J. K., and Zweerink, H. J. (1991) *J. Biol. Chem.* **266,** 98–103
31. Ramage, P., Cheneval, D., Chvei, M., Graff, P., Hemmig, R., Heng, R., Kocher, H. P., Mackenzie, A., Memmert, K., Revesz, L., and Wishart, W. (1995) *J. Biol. Chem.* **270,** 9378–9383
32. Walker, N. P., Talanian, R. V., Brady, K. D., Dang, L. C., Bump, N. J., Ferenz, C. R., Franklin, S., Ghayur, T., Hackett, M. C., Hammill, L. D., Herzog, L., Hugunin, M., Houy, W., Mankovich, J. A., McGuiness, L., Orlewicz, E., Paskind, M., Pratt, C. A., Reis, P., Summani, A., Terranova, M., Welch, J. P., Xiong, L., Möller, A., Tracey, D. E., Kamen, R., and Wong, W. W. (1994) *Cell* **78,** 343–352
33. Rosenberg, M., Ho, Y., and Shatzman, A. (1983) *Methods Enzymol.* **101,** 123–138
34. Chang, A. C. Y., and Cohen, S. N. (1978) *J. Bacteriol.* **134,** 1141–1156
35. Zimmerman, M., Yurewicz, E., and Patel, G. (1976) *Anal. Biochem.* **70,** 258–262
36. Ayala, J. M., Yamin, T.-T., Egger, L. A., Chin, J., Kostura, M. J., and Miller, D. K. (1994) *J. Immunol.* **153,** 2592–2599
37. Gu, Y., Wu, J., Faucheu, C., Lalanne, J., Diu, A., Livingston, D. J., and Su, M. S. (1995) *EMBO J.* **14,** 1923–1931

Additions and Corrections

Vol. 271 (1996) 21853–21858

Stability and oligomeric equilibria of refolded interleukin-1β converting enzyme.

Robert V. Talanian, Luan C. Dang, Catherine R. Ferenz, Maria C. Hackett, John A. Mankovich, Jeffrey P. Welch, Winnie W. Wong, and Kenneth D. Brady

Page 21856, Fig. 3*C*: The molecular weight standards are incorrect. The correct numbers, descending along the *left side* of the figure, should be 29, 20.4, 14, 6.1, and 3.5. The data of this figure are explained correctly in the text. This does not change any of the conclusions in the paper.

Enzymology:

Stability and Oligomeric Equilibria of Refolded Interleukin-1 β Converting Enzyme

Robert V. Talanian, Luan C. Dang, Catherine R. Ferenz, Maria C. Hackett, John A. Mankovich, Jeffrey P. Welch, Winnie W. Wong and Kenneth D. Brady

J. Biol. Chem. 1996, 271:21853-21858.
doi: 10.1074/jbc.271.36.21853
